

Analysis and reduction of a detailed chemical kinetic model of 1-pentene combustion at high temperature

FENG HongQing*, MENG XiangFeng, CHENG Gang & WANG MeiYing

College of Pipeline and Civil Engineering, China University of Petroleum, Qingdao 266580, China

Received July 26, 2012; accepted October 11, 2012

A new reduced chemical kinetic model of 1-pentene is developed based on a detailed chemical kinetic model of 1-pentene at high temperature (194 species and 1266 reactions). By means of sensitivity and flow rate analyses, 32 important reactions are determined, on the basis of which a reduced chemical kinetic model consisting 50 species and 251 reactions is proposed through addition of other important species and reactions. The results show that the simulated cylinder pressure and temperature calculated using the reduced model agree well with those from the detailed model. The reduced model requires less computing time than the detailed model, which enables coupled computation of the chemical kinetic model with computational fluid dynamics.

1-pentene, reduced chemical kinetic model, sensitivity analysis

Citation: Feng H Q, Meng X F, Cheng G, et al. Analysis and reduction of a detailed chemical kinetic model of 1-pentene combustion at high temperature. *Chin Sci Bull*, 2013, 58: 1072–1078, doi: 10.1007/s11434-012-5616-y

Reduced kinetic mechanisms are very important for simulating hydrocarbon fuel combustion processes [1]. A significant amount of alkenes is present in gasoline in China, and these are important primary products from the oxidation of alkanes [2]. The alkene weight content of 93 gasoline produced by China National Petroleum Corporation (CNPC) and Sinopec Group refineries in 2010 is presented in Table 1.

Alkenes that contain 5 carbon atoms (C5) are the most common in 93 gasoline. However, in the chemical kinetic models used to simulate alkene combustion, very few model alkenes containing more than four carbon atoms. Most studies concerning alkenes focus on ethylene, propene, and butene, which are actually not present in gasoline [3,4]. Touchard et al. [5] calculated the oxidation mechanisms of 1-pentene at high and low temperature based on the oxidation mechanism of short alkenes by an automatic mechanism generation tool software. The oxidation of 1-pentene has been experimentally studied by Ribaucour et al. [6,7] in a rapid compression machine between 600 and 900 K and by Prabhu et al. [8] in a plug flow reactor between 600 and 800 K. Alatorre et al. [9] investigated the oxidation

Table 1 Content of alkenes in 93# Gasoline in China

Carbon number	Sinopec (%)	CNPC (%)
C4	2.21	0.59
C5	6.85	4.94
C6	2.75	4.46
C7	0.89	3.31
C8	0.24	1.92
C9	0.22	1.19
C10	0.31	0.39
C11	0.00	0.00
Total	13.49	16.8

of a fuel-rich flame containing 1-pentene, oxygen and argon at low pressure.

In this paper, a reduced chemical kinetic model of combustion of 1-pentene at high temperature based on the oxidation mechanism developed by Touchard et al. [2] is presented. Temperature sensitivity and material generation rate analyses were used to obtain the model. The distribution of oxidized products from 1-pentene and the effect of important species were also considered. Comparison with results obtained using the detailed chemical kinetic model show that the reduced chemical kinetic model can accurately

*Corresponding author (email: fenghongqing@upc.edu.cn)

ly predict the heat released from the combustion of 1-pentene. The reduced model requires less computational time than the detailed one, and allows the multi-dimensional computational fluid dynamics (CFD) numerical simulation of alkenes.

1 Developing the reduced chemical kinetic model

1.1 The detailed chemical kinetic model

The oxidation mechanism of 1-pentene at high temperature reported by Touchard et al. [5] is used as the detailed chemical kinetic model in this work. This model was generated by the automatic mechanism generation tool software, and contains 194 species and 1266 reactions (denoted 194/1266).

The detailed model is composed of three parts: (1) A comprehensive primary mechanism. This part contains 179 reactions of 1-pentene or the radicals that it produces. (2) A combined secondary mechanism. This part contains 298 reactions, including the consumption reactions of the molecular products produced in the primary mechanism. (3) A base reaction. This part contains 789 reactions, including all the reactions of C0-C2 molecules and radicals.

This mechanism has been verified by shock tube experiments, and the ignition delay obtained experimentally accords with simulated results [2]. However, this mechanism is so large that if it is coupled with multidimensional computational fluid dynamics numerical simulation, the computation time becomes unfeasible. As a result, this detailed model should be reduced. Developing a reduced chemical kinetic model that keeps the heat released by the reaction, reaction pathways of important products and reaction rates consistent with the actual process are necessary to better understand the mechanism and allow the coupled computation of the chemical kinetic reaction with computational fluid dynamics.

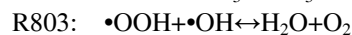
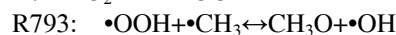
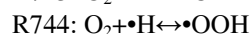
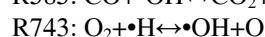
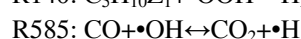
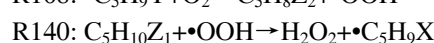
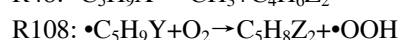
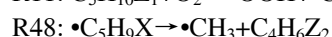
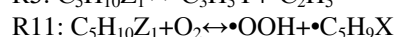
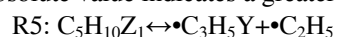
1.2 Reducing the detailed reaction mechanism

Many methods to reduce chemical kinetic models have been developed such as the sensitivity analysis method, quasi-stationary approximation, finite rate theory of balance control, and software that automatically generates a reduced reaction mechanism [10,11]. Herein, the sensitivity analysis method was used to reduce the chemical kinetic model of 1-pentene at high temperature developed by Touchard et al. [2].

The chemical kinetic calculation software developed by the Sandia National Laboratories Combustion Research Facility is used in this paper. This version adds an individual module to calculate the homogeneous charge compression ignition (HCCI) engine, and embeds a zero dimension single-zone model as the physical model of an engine. Be-

cause comparison with actual engine combustion characteristics is not involved in the reduction of the mechanism, the homogeneous charge compression ignition module was used, and the heat transfer between cylinder walls was not considered to save computing resources.

Figure 1 shows the results of temperature sensitivity analysis of the detailed mechanism for different equivalence ratios (ϕ), while Table 2 shows the operating parameters of the HCCI engine. The positive sensitivity coefficient means that if the reaction pre-exponential factor A increases (i.e., the reaction rate increases), the temperature will rise, and conversely the temperature will fall if A decreases. A larger absolute value indicates a greater effect on the temperature.



The reactions in Figure 1 are shown below.

Table 2 Operating parameters of the HCCI engine

Parameter	Value
Compression ratio	16.5
Clearance volume (cm ³)	103.3
Rod crank ratio	3.7
Speed (r/min)	1000
Intake valve close angle (°CA)	-142
Initial temperature (K)	600
Initial pressure (kPa)	106.5
Equivalence ratio	0.2–1.0

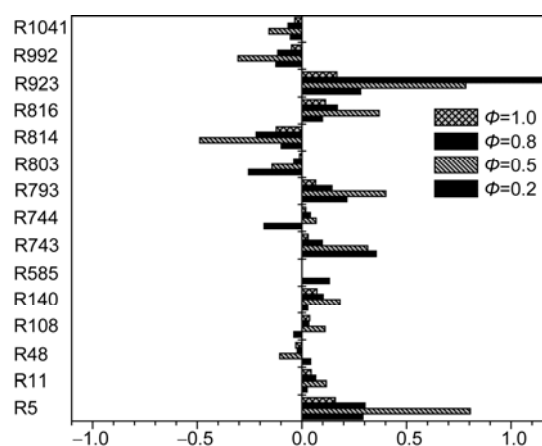


Figure 1 Temperature sensitivity analysis of the reaction rate for different equivalence ratios.

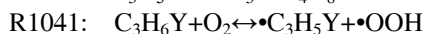
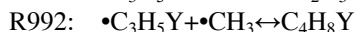


Figure 1 shows that R923 has the largest temperature sensitivity of the reactions. R5, R743, R793, R814, R816 and R923 are also significantly influenced by temperature. For the reaction $\bullet\text{C}_3\text{H}_9\text{X} \rightarrow \bullet\text{CH}_3 + \text{C}_4\text{H}_6\text{Z}_2$, when $\phi = 0.2$, the temperature sensitivity coefficient is positive, but when $\phi > 0.2$, the coefficient is negative. Conversely, for the reactions $\bullet\text{C}_3\text{H}_9\text{Y} + \text{O}_2 \rightarrow \text{C}_5\text{H}_8\text{Z}_2 + \bullet\text{OOH}$ and $\text{O}_2 + \bullet\text{H} \leftrightarrow \bullet\text{OOH}$, when $\phi = 0.2$, the temperature sensitivity coefficient is negative, but when $\phi > 0.2$, the coefficient is positive. The influence of temperature on these three reactions changes direction as ϕ changes. The reaction $\text{CO} + \bullet\text{OH} \leftrightarrow \text{CO}_2 + \bullet\text{H}$ only proceeds when $\phi = 0.2$. The influence of temperature on the reactions is the largest when $\phi = 0.5$.

Figure 2 shows the temperature sensitivity of the 10 reactions with the largest sensitivity coefficients when $\phi = 0.5$ and 1. Figure 2(a) shows that the largest temperature sensitivity for every reaction is at 0.191 s and about 1300 K. Figure 2(b) shows that reaction R923 has the largest temperature sensitivity of the reactions. Except for R923, the influence of temperature on the other reactions changes direction before and after combustion. These reactions include

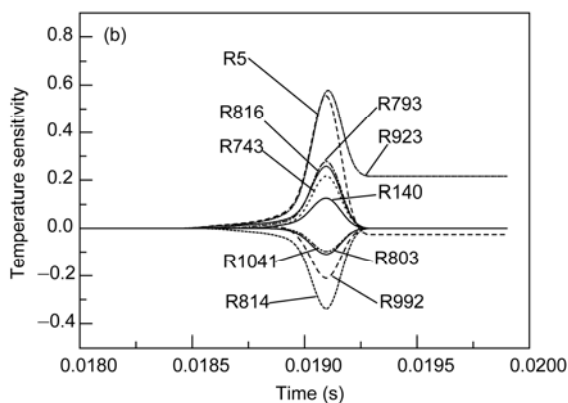
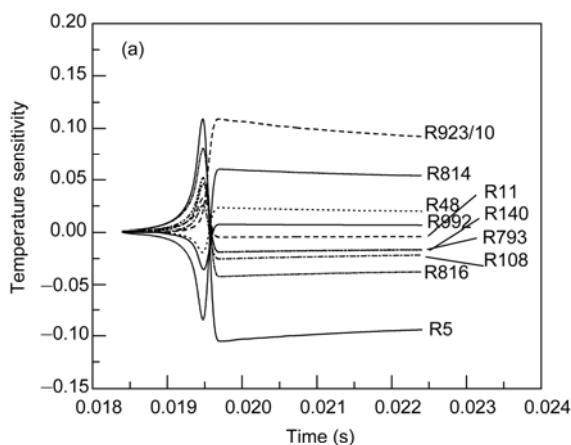


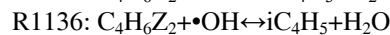
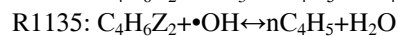
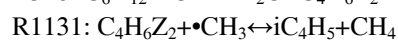
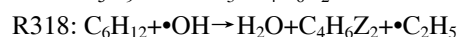
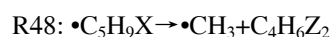
Figure 2 Temperature sensitivity of the reaction rate (a) $\phi = 0.5$ and (b) $\phi = 1.0$ (the temperature sensitivity of R923 has been divided by 10).

the single molecule initial reaction R5 that produces allyl and ethyl species, dimolecular initial reaction R11 that produces the isomeride $\bullet\text{C}_5\text{H}_9\text{X}$ from the pentenyl, β bond cleavage R48, oxidation R108, hydrogen abstraction R140, and basic reactions R793, R814, R816, R923, R922.

Comparing Figure 2(a) and (b), the maximum reaction temperature sensitivity is delayed as ϕ increases. This is because that the ignition delay increases and the maximum temperature takes longer to reach as ϕ increases.

Sensitivity analysis shows that the rates of the 15 reactions shown above are significantly affected by the temperature of the system. However, these 15 reactions are not sufficient to describe the oxidation of 1-pentene at high temperature because some important reactions have not been included, such as the reaction $\text{C}_5\text{H}_{10}\text{Z}_1 + \bullet\text{H} \rightarrow \text{H}_2 + \bullet\text{C}_5\text{H}_9\text{X}$ and $\text{C}_5\text{H}_{10}\text{Z}_1 + \text{OH} \rightarrow \text{H}_2\text{O} + \bullet\text{C}_5\text{H}_9\text{X}$ that produce the important intermediate product 1,3-butadiene, and the reaction $\bullet\text{C}_2\text{H}_5 \leftrightarrow \text{C}_2\text{H}_4 + \bullet\text{H}$ that produces the main primary product ethylene. A material flow analysis of 1-pentene at 1222 K with $\phi = 1$ and 50% conversion rate is shown in Figure 3.

It can be seen that, except for the above reactions, the oxidation of 1-pentene at high temperature also includes the reaction $\bullet\text{H} + \text{C}_5\text{H}_{10}\text{Z}_1 \leftrightarrow \bullet\text{C}_5\text{H}_{11}$, which produces pentyl. These reactions are summarized in Table 3.



The reactions that were identified as being important by sensitivity and flow analyses were used to form a model with 32 reactions. The primary products of these 32 reactions, the important radicals that the high temperature reaction requires and other important intermediate products of combustion such as formaldehyde, methanol and the combustion products CO, CO₂, and H₂O are presented in Table 4. The production rates of these 47 species were analyzed

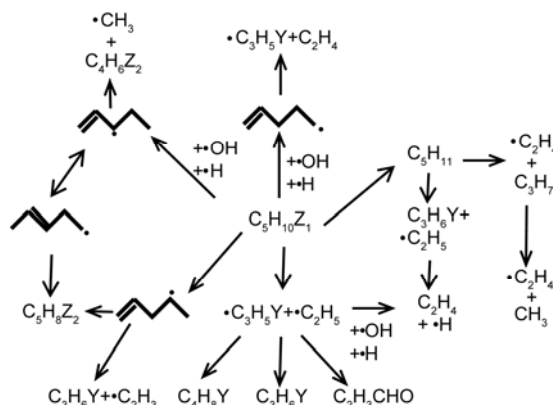


Figure 3 Material flow analysis at 1222 K.

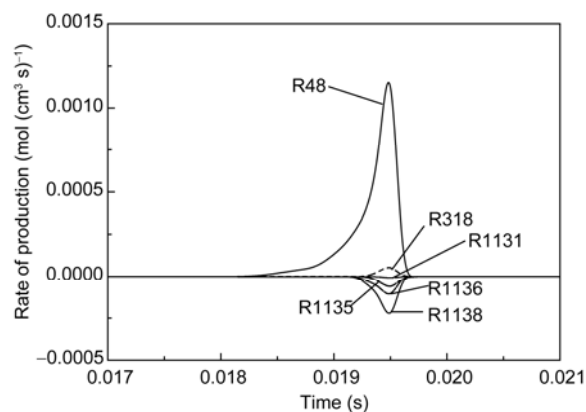
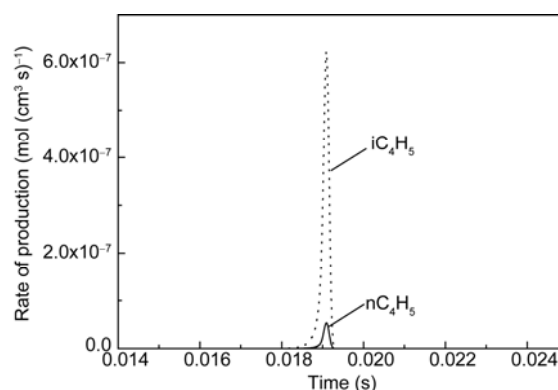
Table 3 Reactions added to the material flow analysis

Number	Reaction
1	$C_5H_{10}Z_1 + \bullet H \rightarrow H_2 + \bullet CH_2CHCH_2CH_2CH_2$
2	$C_5H_{10}Z_1 + \bullet OH \rightarrow H_2O + \bullet CH_2CHCH_2CH_2CH_2$
3	$C_5H_{10}Z_1 + \bullet H \rightarrow H_2 + \bullet CH_2CHCHCH_2CH_3$
4	$C_5H_{10}Z_1 + \bullet OH \rightarrow H_2O + \bullet CH_2CHCHCH_2CH_3$
5	$C_5H_{10}Z_1 + \bullet H \rightarrow H_2 + \bullet CH_2CHCH_2CHCH_3$
6	$C_5H_{10}Z_1 + \bullet OH \rightarrow H_2O + \bullet CH_2CHCH_2CHCH_3$
7	$\bullet CH_2CHCH_2CHCH_3 \rightarrow \bullet H + C_5H_8Z_2$
8	$\bullet CH_2CHCH_2CHCH_3 \rightarrow \bullet C_2H_3 + C_3H_6Y$
9	$\bullet CH_2CHCH_2CH_2CH_2 \rightarrow \bullet C_3H_5 + C_2H_4$
10	$\bullet H + C_5H_{10}Z_1 \leftrightarrow \bullet C_5H_{11}$
11	$\bullet C_2H_5 \leftrightarrow C_2H_4 + \bullet H$
12	$\bullet CH_2CHCHCH_2CH_3 \leftrightarrow \bullet CH_3CHCHCH_2CH_2$
13	$\bullet C_3H_5 + H \leftrightarrow C_3H_6Y$
14	$\bullet C_5H_{11} \rightarrow \bullet C_2H_5 + C_3H_6Y$
15	$\bullet C_5H_{11} \rightarrow \bullet C_3H_7 + C_2H_4$
16	$\bullet C_3H_7 \leftrightarrow \bullet CH_3 + C_2H_4$

separately. The production rate for 1,3-butadiene is shown in Figure 4.

Figure 4 shows that the major positive reaction of 1,3-butadiene is $\bullet C_5H_9X \rightarrow \bullet CH_3 + C_4H_6Z_2$, and the major negative reaction is $C_4H_6Z_2 + \bullet OH \leftrightarrow CH_3CHO + \bullet C_2H_3$. Hexene (C_6H_{12}) is mainly produced by the dehydrogenation of hexyl, and the reaction that produces hexyl (the reaction of pentene and methylic) is an important branch of the oxidation of pentene. However, because the oxidation of hexene occurs in parallel with the oxidation of pentene, the reaction R318 was not considered to focus on the oxidation of pentene at high temperature.

Figure 5 shows the generation rates of iC_4H_5 and nC_4H_5 . It can be seen that the total production rate of these two species is very small, around 10^{-7} . Because the effect of temperature on this reaction is small, only the reactions

**Figure 4** Material flow analysis for 1,3-butadiene with $\phi = 1$. The reactions in the Figure 4 are shown below.**Figure 5** Generation rate of iC_4H_5 and nC_4H_5 .

R48, R1134, R1137, R1138 and R1200 were retained.

Overall, the oxidation of 1-pentene at high temperature has been reduced from a model that contains 194 species and 1266 reactions to a model that contains 50 species and 251 reactions through the method described above.

Table 4 Species in the initial model

Primary product	Important intermediate product	Radical	Combustion product
$\bullet C_2H_3$	H_2	C_3H_3	$\bullet H$
C_2H_4	HCHO	CH_3CHO	O
$\bullet C_2H_5$	H_2O_2	COC_2H_3	$\bullet OH$
$\bullet C_3H_5$ (allyl)	CHCH	C_2H_4O	$\bullet CH_3$
C_2H_3CHO	CH_2CO	C_3H_4	$\bullet OOH$
C_3H_6Y	CH_4	$CH_2=CHCH_2$	$\bullet CHO$
$C_4H_6Z_2$ (1,3-butadiene)	CH_2OH	$CH=CHCH_3$	
$\bullet C_3H_7$ (n,i)	CH_3O	C_2H_6Y	
C_4H_8Y	CH_2CHO	C_2H_5CHO	
$CH_2=CHCH=CHCH_3$	CH_3OH	$\bullet C_4H_7$	
$\bullet CH_2=CHCHCH_2CH_3$	CH_3OO	CH_3CO	
$\bullet CH_2=CHCH_2CH_2CH_2$			
$\bullet CH_2=CHCH_2CHCH_3$			
$\bullet CH_3CH=CHCH_2CH_2$			
$\bullet C_5H_{11}$			

2 Results and discussion

To validate the reduced model, both the reduced and detailed models were used to perform calculations under the same boundary conditions, and the calculation results were compared. The operating parameters for the HCCI engine with ϕ of 0.2, 0.5, 0.8 and 1.0 are shown in Table 2.

2.1 Comparative analysis of cylinder pressure and temperature

Figure 6 shows the cylinder pressure traces determined using the reduced and detailed models for different ϕ . It can be seen that, for each ϕ , the combustion phase of the reduced model agrees well with the combustion phase of the detailed model, except for the slightly lower maximum pressure. The two curves coincide during early and late combustion. Meanwhile, the reduced mechanism can correctly predict the variation in combustion with changes in ϕ .

Figure 7 shows that the maximum pressure increases with ϕ . The cylinder temperature at different ϕ calculated using the two different models is shown in Figure 8. The cylinder temperatures calculated using the two models generally agree well, except the temperature calculated using the reduced model is lower for late combustion. The reason

for this may be that the reduced model ignores some exothermic reactions that are very active in the initial combustion but weak in the late combustion.

2.2 Comparative analysis of the important processes during combustion of 1-pentene

The molar concentration of 1-pentene and several important species when $\phi = 1$ are presented in Figure 9. Figure 9(a) shows that the combustion of 1-pentene calculated using the reduced model is consistent with that calculated using the detailed model. That is, the reduced model can correctly simulate the combustion process of 1-pentene.

The change of $\bullet\text{OH}$ during combustion is shown in Figure 9(b). The combustion phase calculated using the reduced and detailed models agree well, except that in the later stage of combustion (above 1200 K), the concentration of $\bullet\text{OH}$ determined by the reduced model increases slowly, so it is lower than that estimated by the detailed model. Figure 9(c) shows the change in the molar concentration of $\bullet\text{OOH}$ during combustion. The results calculate for the reduced and detailed models are fairly consistent. Compared with the detailed model, the results for the reduced model are higher for the first maximum, but lower for the second maximum of $\bullet\text{OOH}$. Figure 9(d) shows the molar concentration

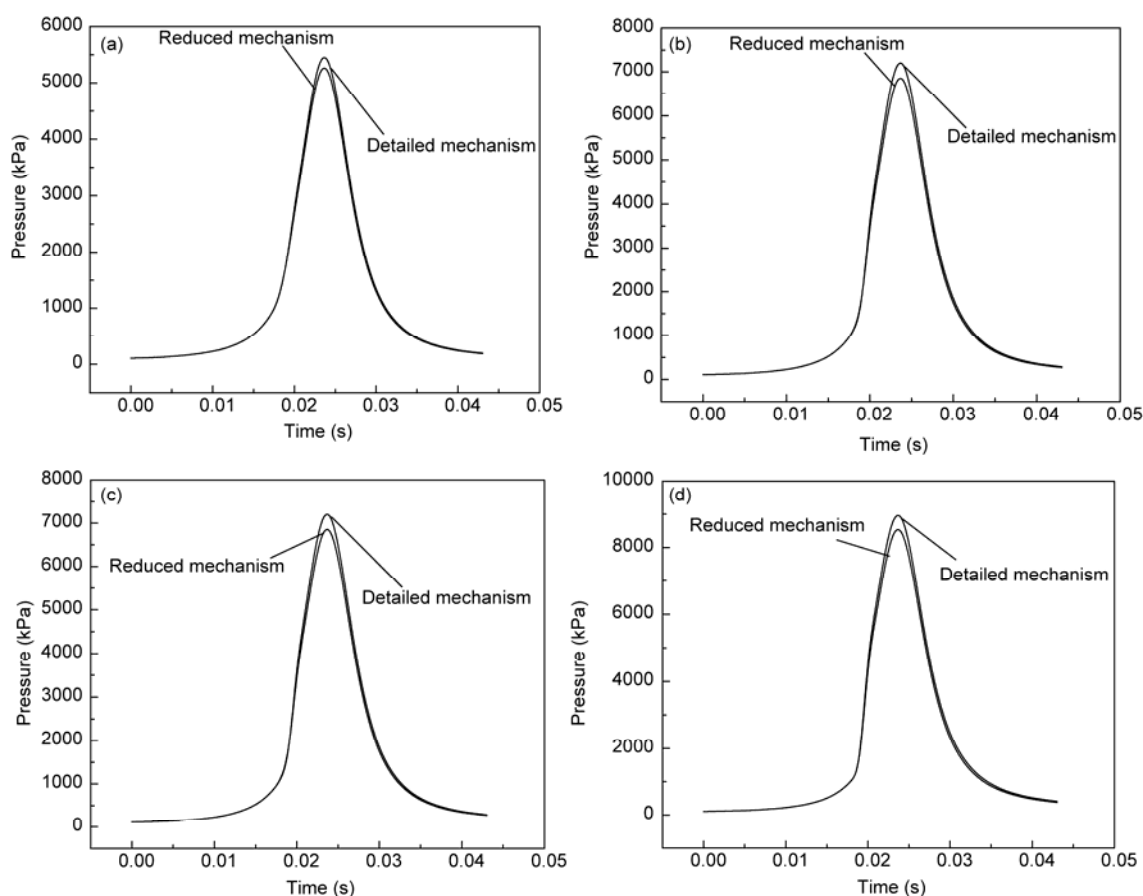


Figure 6 Cylinder pressure for different ϕ (a) $\phi = 0.2$; (b) $\phi = 0.5$; (c) $\phi = 0.8$ and (d) $\phi = 1.0$.

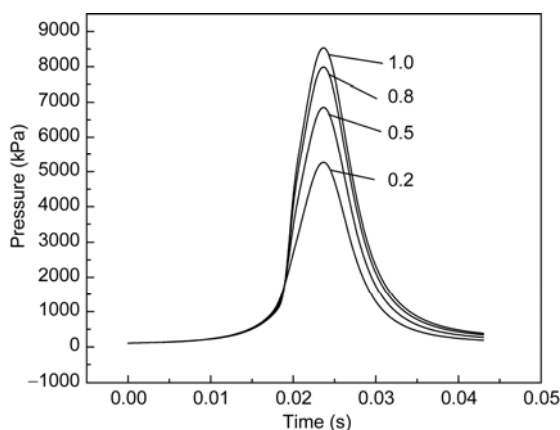


Figure 7 Cylinder pressure of the reduced mechanism.

of CO. The reduced model correctly predicted the trend of CO, except that in the later stage of combustion, the maximum concentration of CO estimated by the reduced model is quite different from that of the detailed mechanism because of a decrease in production rate.

The molar concentration of C_2H_4 during the combustion of 1-pentene is shown in Figure 9(e). Again, the results cal-

culated using the reduced and detailed models coincide. The reduced model can correctly predict the change in the molar concentration of C_2H_4 during combustion.

3 Conclusions

A reduced model for the combustion of 1-pentene at high temperature containing 50 species and 251 reactions has been developed. The model was generated based on 15 elementary reactions obtained from sensitivity, flow and general rate analyses. The cylinder pressure and temperature calculated using the reduced and detailed models are consistent for ϕ of 0.5, 0.8, 1.0 and 1.2. The reduced model can correctly predict changes in cylinder combustion with ϕ . The reduced model can correctly predict the variation in the concentration of important species such as CO, $\bullet OH$, $\bullet OOH$, C_2H_4 , and $C_5H_{10}Z_1$. The results show that the reduced model can simulate the combustion of 1-pentene at high temperature, and significantly reduce the computational time (computational time is about 1/6 of that required for the detailed model). This will enable the coupled computation of the CFD multi-dimensional model with the chemical kinetics model.

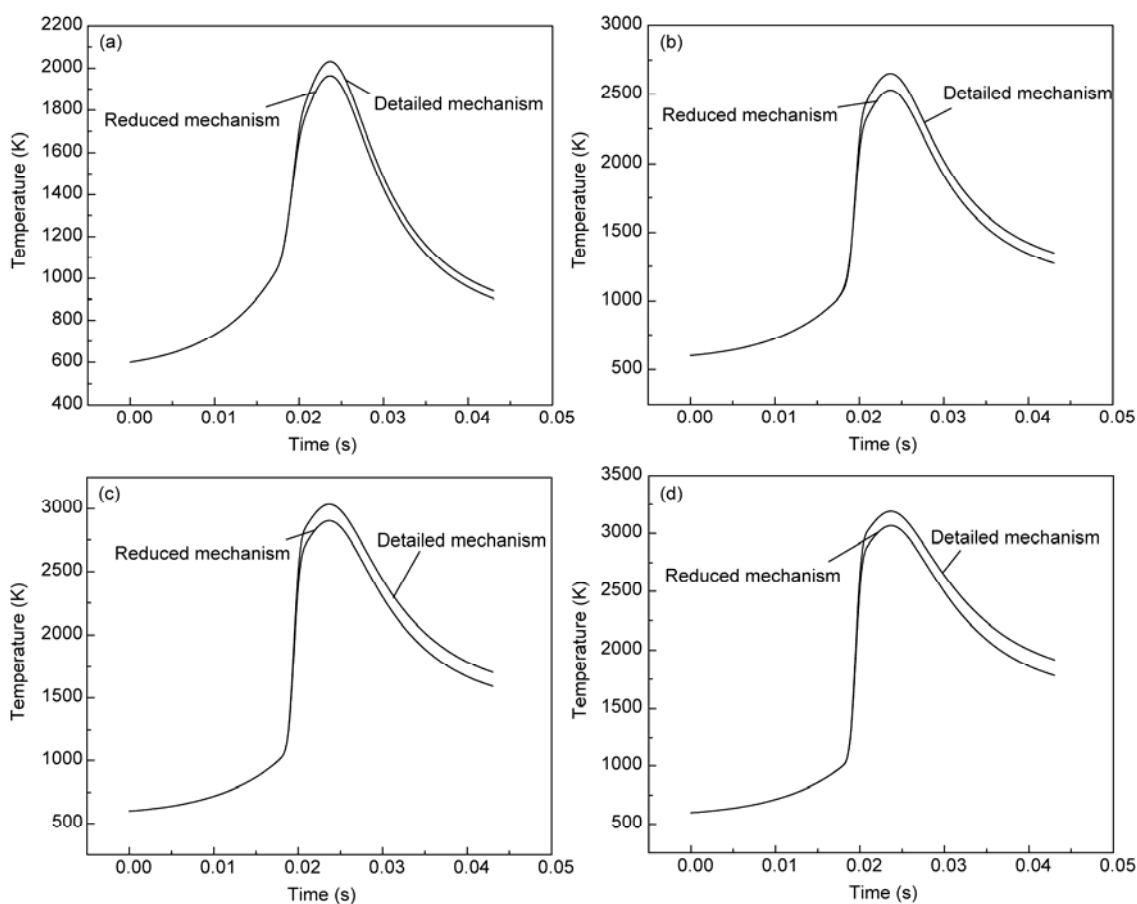


Figure 8 Cylinder temperature for different ϕ calculated using the detailed and reduced models. (a) $\phi=0.2$; (b) $\phi=0.5$; (c) $\phi=0.8$ and (d) $\phi=1.0$.

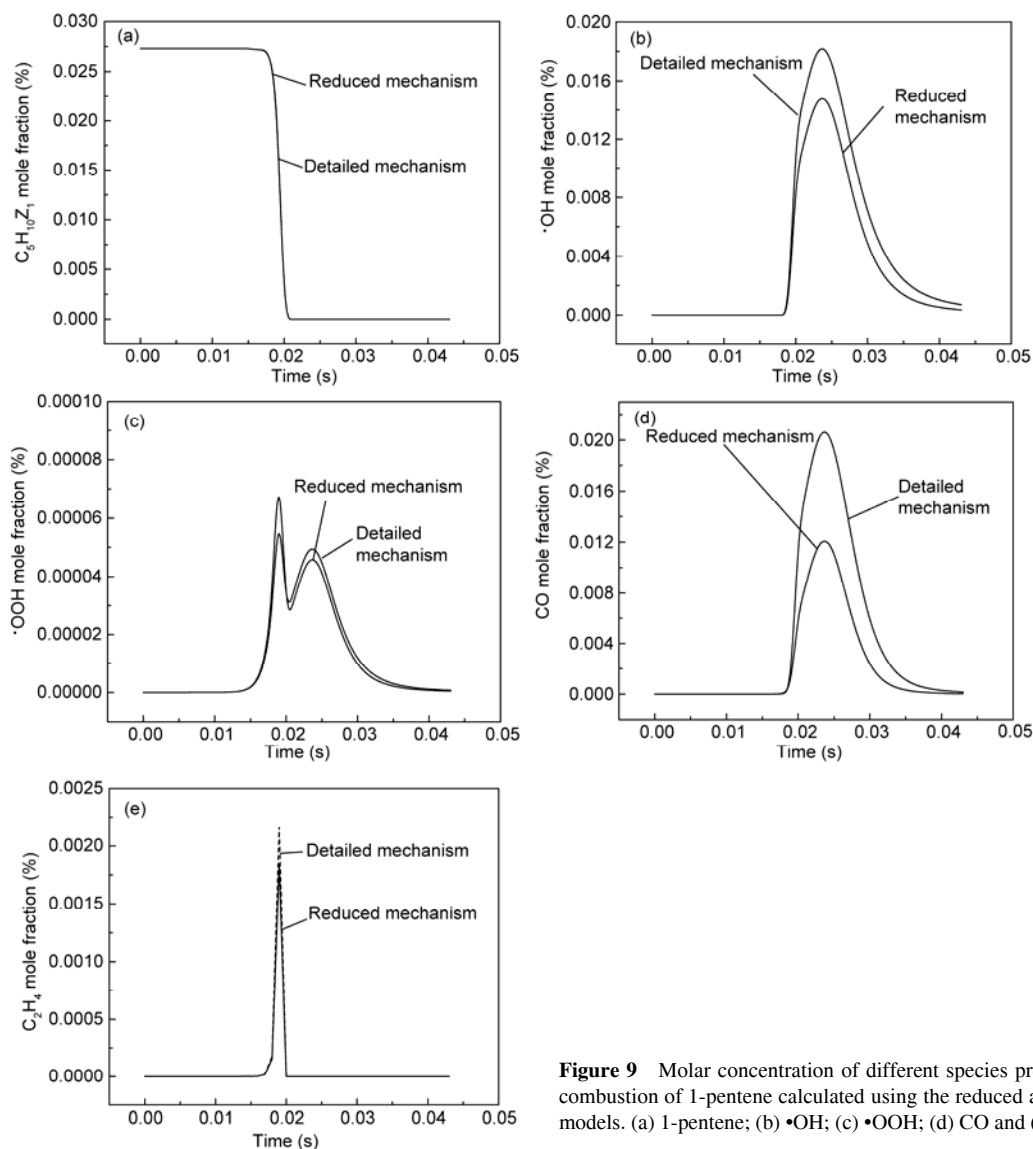


Figure 9 Molar concentration of different species present in the combustion of 1-pentene calculated using the reduced and detailed models. (a) 1-pentene; (b) \bullet OH; (c) \bullet OOH; (d) CO and (e) C_2H_4 .

This work was supported by the National Natural Science Foundation of China (51106181), the State Key Laboratory of Engines in Tianjin University (K2012-06), and Promotive Research Fund for Young and Middle-Aged Scientists of Shandong Province (BS2012NJ012).

- Jiang Y, Qiu R, Fan W C. A kinetic modeling study of pollutant formation in premixed hydrocarbon flames. *Chin Sci Bull*, 2005, 50: 276–281
- Touchard S, Buda F, Dayma G, et al. Experimental and modeling study of the oxidation of 1-pentene at high temperature. *Int J Chem Kinet*, 2005, 37: 451–463
- Heyberger B, Belmekki N, Conraud V, et al. Oxidation of small alkenes at high temperature. *Int J Chem Kinet*, 2002, 34: 666–677
- Heyberger B, Battin-leclerc F, Warth V, et al. Comprehensive mechanism for the gas-phase oxidation of propene. *Combust Flame*, 2001, 126: 1780–1802
- Touchard S, Fournet R, Glaude P A, et al. Computer aided generation of kinetic mechanism-application to the oxidation of large alkenes at low-temperature. In: Chauveau C, Vovelle C, eds. *Proceedings of the European Combustion Meeting*, Orleans, France, 2003. 1–6
- Touchard S, Fournet R, Glaude P A, et al. Modeling of the oxidation of large alkenes at low temperature. *P Combust Inst*, 2004, 30: 1073–1081
- Ribaucour M, Minetti R, Sochet L R. Autoignition of n-pentane and 1-pentene: Experimental data and kinetic modeling. *P Combust Inst*, 1998, 27: 345–351
- Prabhu S K, Bhat R K, Miller D L, et al. 1-pentene oxidation and its interaction with nitric oxide in the low and negative temperature coefficient regions. *Combust Flame*, 1996, 104: 377–390
- Alatorre G G, Böhm H, Burak A, et al. Experimental and modelling study of 1-pentene combustion at fuel-rich conditions. *Phys Chem*, 2001, 215: 981–995
- Huang H Z, Su W H. Development and optimization of a new reduced chemical kinetics for n-heptane combustion (in Chinese). *J Eng Thermophys*, 2006, 27: 883–886
- Zhao C P, Chen S Q, Li Y L, et al. Reduction of a detailed chemical kinetics model of n-heptane combustion and its validity analysis (in Chinese). *Trans Chin Soc Inter Combust Engines*, 2008, 26: 346–352

Open Access This article is distributed under the terms of the Creative Commons Attribution License which permits any use, distribution, and reproduction in any medium, provided the original author(s) and source are credited.